

Three-body mechanisms in the ${}^3\text{He}(e, e' p)$ reactions at high missing momentum

J. M. Laget

CEA-Saclay, Service de Physique Nucléaire, F-91191 Gif-sur-Yvette, Cedex, France and
Thomas Jefferson National Accelerator Facility, Newport News, Virginia 23606, USA

(Received 4 October 2004; published 10 August 2005)

A particular three-body mechanism is responsible for the missing strength that has been reported in ${}^3\text{He}(e, e' p)$ reactions at missing momentum above 700 MeV/c. It corresponds to the absorption of the virtual photon by a nucleon at rest which subsequently propagates on shell and emits a meson which is reabsorbed by the pair formed by the two other nucleons. Its amplitude, which is negligible in photon-induced reactions as well as in the electroproduction of an on-shell meson, becomes maximal in the quasifree kinematics ($X = 1$). This mechanism relates the amplitude of the ${}^3\text{He}(e, e' p)^2\text{H}$ reaction to the amplitude of pd elastic scattering at backward angles.

DOI: [10.1103/PhysRevC.72.024001](https://doi.org/10.1103/PhysRevC.72.024001)

PACS number(s): 24.10.-i, 25.10.+s, 25.30.Dh, 25.30.Fj

The recent study at the Thomas Jefferson National Accelerator Facility (JLab) of the ${}^3\text{He}(e, e' p)$ reactions [1,2] represents a textbook result. One-, two-, and three-body mechanisms have been disentangled in a single experiment. The two-body breakup channel, Fig. 1, is particularly illuminating in this respect. One-body mechanisms, where the electron interacts with a single nucleon and the deuteron is spectator (plane wave), dominate below missing momentum $p_m \simeq 300$ MeV/c (the momentum of the outgoing deuteron). For missing momenta between 300 and 700 MeV/c, nucleon-nucleon final state interactions (FSI) take over [3], while two-body meson exchange currents (MEC) and Δ formation contribute only at the level of 20%. However, the recombination of one of the two active nucleons with the third nucleon to form the outgoing deuteron strongly reduces the corresponding cross section at high p_m . Independent evaluations Refs. [3,4] of the contributions of one- and two-body mechanisms miss by one order of magnitude the experiment at $p_m \simeq 1$ GeV/c. Here, three-body mechanisms dominate and restore the agreement with data. The first reason is that sequential meson exchange is the more economical way to share the large momentum transfer among the three nucleons. The second reason is that the on-shell nucleon singularity maximizes the contribution of one of these diagrams in the quasielastic kinematics ($X = Q^2/2m\nu = 1$, Q^2 and ν being, respectively, the virtuality and the energy of the virtual photon, while m is the mass of the nucleon), for the same reason [3] that the contribution of nucleon-nucleon rescattering is maximized. The virtual photon is absorbed by a nucleon at rest which subsequently propagates on shell before emitting a meson that is reabsorbed by the two other nucleons. In real photon-induced reactions Refs. [5,6], the corresponding singularity is suppressed by the high-momentum components of the nuclear wave function since, for kinematical reasons, the absorption by a nucleon at rest is forbidden. Also, the intermediate nucleon cannot be on shell in the electroproduction of an on-shell meson. The corresponding three-nucleon amplitude was switched off [5] in my previous evaluation [3]. This report is devoted to the proper evaluation of the contribution of this diagram and its on-shell singularity.

The method [7] is based on the expansion of the reaction amplitude in terms of a few relevant diagrams, which are computed in the momentum space, in the laboratory frame. The kinematics as well as the propagators are relativistic and no angular approximation is made in the evaluation of the loop integrals. The elementary operators that appear at each vertex have been calibrated against the corresponding channels. The method's application to the ${}^3\text{He}(e, e' p)$ channels has been discussed in Refs. [5,8,9] and updated in Ref. [3] to the JLab energy range. A comprehensive summary is given in Ref. [10] for the ${}^4\text{He}(e, e' p)^3\text{H}$ channel.

For the sake of the discussion, I reproduce the expression of the amplitude of the three-body mechanisms [5] for the ${}^3\text{He}(e, e' p)^2\text{H}$ reaction and the main steps of its evaluation as

$$T = i \int \frac{d^3\vec{n}}{(2\pi)^3} \sum_{m_n} T(\gamma^3\text{He} \rightarrow npp) \times \left[\left(\frac{1}{2} m_p \frac{1}{2} m_n \middle| 1m_2 \right) \frac{U_0^D(\vec{n} - \vec{p}_2/2)}{\sqrt{4\pi}} + D \text{ wave} \right], \quad (1)$$

where U_0^D and U_2^D are the S and D components of the final deuteron wave function for the Paris potential [11], and where (\vec{n}, m_n) and (\vec{p}, m_p) are, respectively, the momenta and magnetic quantum numbers of the neutron and the proton which form the final deuteron. The four momenta of the incoming photon and the outgoing proton and deuteron are, respectively, (ν, \vec{k}) , (E_1, \vec{p}_1) , and (E_2, \vec{p}_2) . Only the positive energy part of the nucleon propagators is retained, and the integral over the energy of the neutron picks the pole in its propagator and puts it on shell.

The three-body break-up amplitude $T(\gamma^3\text{He} \rightarrow npp)$ corresponds to a two-loop diagram, and the integral runs over the four momenta of the two nucleons which do not absorb the photon. Again the energy integration picks their poles and puts them on shell. After changing the variables of integration, we are left with a sixfold integration over the relative (\vec{q}) and the

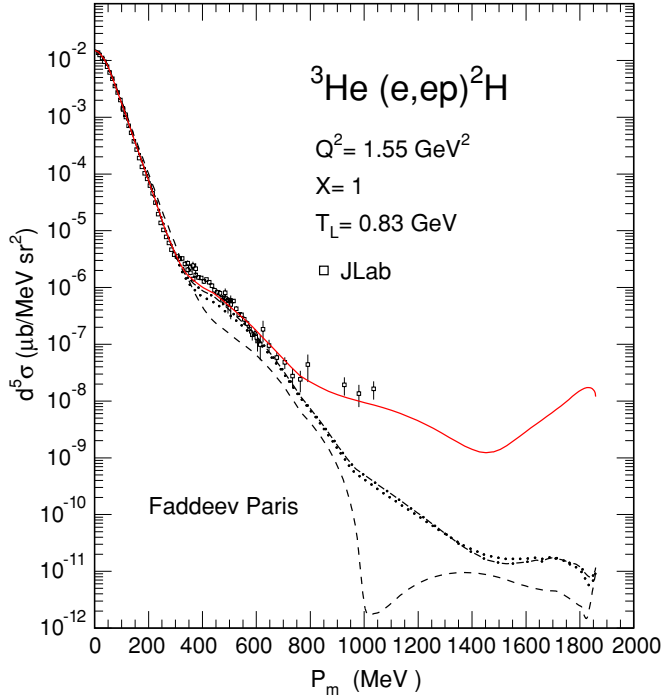


FIG. 1. (Color online) Momentum distribution in the ${}^3\text{He}(e, e'p){}^2\text{H}$ reaction at $E_e = 4.795$ MeV, $X = 1$ and $Q^2 = 1.55$ GeV 2 . Dashed line: plane wave. Dotted line: two-body FSI included. Dash-dotted line: two-body FSI, MEC, and Δ production included. Full line: three-body mechanisms included. The data are from Ref. [1].

total ($-\vec{p}'$) momenta of these two nucleons, that is,

$$\begin{aligned}
 T(\gamma^3\text{He} \rightarrow npp) &= -\sqrt{3} \sum_{\Lambda} \left(1\Lambda \frac{1}{2} m'_p \left| \frac{1}{2} m_i \right. \right) \int \frac{d^3 \vec{p}'}{(2\pi)^3} \frac{1}{\sqrt{4\pi}} \\
 &\times \frac{\chi_0^{T=0}(\vec{p}')}{q_\pi^2 - m_\pi^2 + i\epsilon} T_{\gamma p}(\vec{k}, \vec{p}' m'_p \rightarrow \vec{q}_\pi, \vec{n} m_n) \\
 &\times T_{\pi^+(np)_0}(\vec{q}_\pi, -\vec{p}' \Lambda \rightarrow \vec{p} m_p, \vec{p}_1 m_1), \quad (2)
 \end{aligned}$$

where (\vec{p}', m'_p) and $(-\vec{p}', \Lambda)$ are, respectively, the momenta and the magnetic quantum numbers of, respectively, the proton on which the pion is photoproduced and the pair which absorbs it.

The full antisymmetrized three-body wave function [12] is the solution of the Faddeev equation for the Paris potential. It is expanded on a basis where two nucleons couple to angular momentum L , spin S , and isospin T , the third nucleon moving with an angular momentum l . A very good approximation [9] is to factorize each component into a product, $\Phi_{Li}^T = U_L^T(q)\chi_l^T(p)$, of two wave functions which describe, respectively, the relative motion of the two nucleons inside the pair and the motion of the third. Since pion absorption by a $T = 1$ pair is strongly suppressed Refs. [13,14], only absorption by a $T = 0$ pair is retained. This prevents the formation of the Δ in the pion electroproduction elementary amplitude, since the total isospin of the pd final state is $T = 1/2$. The three

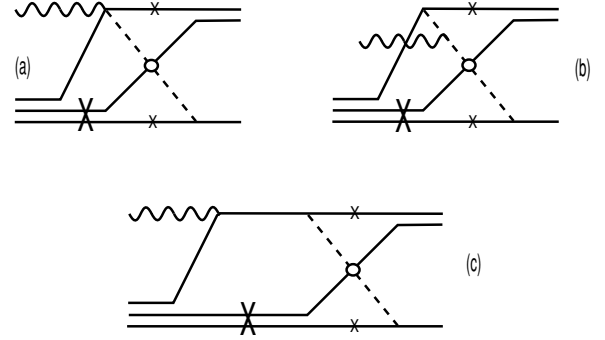


FIG. 2. Three-body graphs. Nucleons put on shell by the integration over the energies are marked by a cross. Dashed lines represent π .

relevant Born terms lead to the three-body graphs depicted in Fig. 2.

In the contact (a) and the photoelectric (b) graphs, which were retained in Refs. [3,5], the only singularity comes from the pole in the pion propagator. I refer to [5] for the details of its treatment and of the choice of the matrix elements of the various elementary amplitudes which enter Eq. (2). The nucleon Born term (c) exhibits an additional singularity which needs a different treatment. After expanding the pion electroproduction amplitude $T_{\gamma p \rightarrow n\pi^+}^B$ and retaining the nucleon Born term, the corresponding part of the three-body breakup amplitude takes the form

$$\begin{aligned}
 T^N(\gamma^3\text{He} \rightarrow npp) &= -\frac{3}{2} \frac{eg_{\pi NN}\sqrt{6}}{2m} \sum_{\Lambda} \left(1\Lambda \frac{1}{2} m'_p \left| \frac{1}{2} m_i \right. \right) \\
 &\times G_M^p(Q^2) \left[\frac{(m_n | \vec{\sigma} \cdot \vec{q}_\pi \vec{\sigma} \cdot \vec{k} \times \vec{\epsilon} | m'_p)}{q_\pi^2 - m_\pi^2} \right. \\
 &\times T_{\pi^+(np)_0}(\vec{q}_\pi, 0\Lambda \rightarrow \vec{p} m_p, \vec{p}_1 m_1) \left. \right]_{\vec{p}'=0} \\
 &\times \int \frac{d^3 \vec{p}'}{(2\pi)^3} \frac{1}{\sqrt{4\pi}} \frac{\chi_0^{T=0}(\vec{p}')}{2E_N(p_N^0 - E_N + i\epsilon)}, \quad (3)
 \end{aligned}$$

where the pion propagator, the pion absorption amplitudes, and the spin-momentum part of the nucleon Born amplitude [15,16] have been factorized out of the integral, which can be expressed in a compact analytic form according to Ref. [7]. Besides π^+ exchange, π^0 exchange contributes also, and the combination of the two amplitudes leads to the factor $3/2$. The on-shell and off-shell energies of the intermediate nucleon are, respectively, $E_N = \sqrt{(\vec{p}' + \vec{k})^2 + m^2}$ and $p_N^0 = \nu + m_{3\text{He}} - \sqrt{\vec{p}'^2 + 4m^2}$. Equation (3) displays the transverse (magnetic) part of the current. Its longitudinal (Coulomb) part exhibits a similar form but contributes weakly to the differential cross section at the high-virtuality Q^2 relevant to this experiment.

As in the NN scattering amplitude [3], the singular (on-shell) part of the integral exhibits a sharp maximum, while its principal (off-shell) part strictly vanishes, in the quasielastic

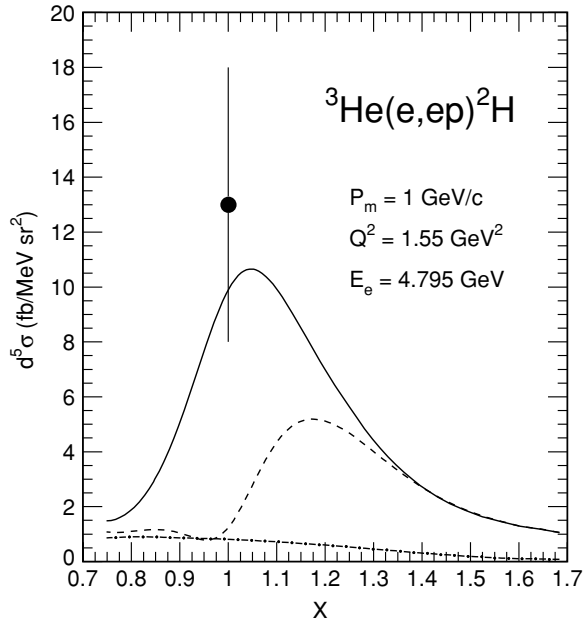


FIG. 3. Angular distribution of the deuteron emitted with a constant momentum $p_m = 1$ GeV/c in the ${}^3\text{He}(e, e' p){}^2\text{H}$ reaction when $Q^2 = 1.55$ GeV 2 and $E_e = 4.795$ GeV. Dash-dotted line: without nucleon Born term [Fig. 2(c)] in the three-body amplitude. Dashed line: principal part of the nucleon Born term included. Full line: singular and principal part of the nucleon Born term included. Datum is from Ref. [1].

kinematics at $X = 1$ (Fig. 3). Here, the virtual photon is absorbed by a proton at rest in ${}^3\text{He}$ which propagates on shell before emitting a (off-shell) pion which is reabsorbed by the pair, formed by the two other nucleons, also at rest in ${}^3\text{He}$. This justifies the factorization of the elementary matrix elements, as well as the pion propagator, in Eq. (3) and their evaluation assuming that the active nucleon and the spectator deuteron are at rest in ${}^3\text{He}$. This is an accurate and parameter-free way to evaluate the ninefold integral, Eq. (1), since it relies on the low-momentum component of the ${}^3\text{He}$ wave function and on-shell elementary matrix element which have been calibrated independently against the corresponding reactions. For instance, Eqs. (1)–(3) relate the two-body disintegration of ${}^3\text{He}$ to backward pd elastic scattering. From studies performed at Saturne and Dubna, we know it is dominated by the exchange of an interacting πN pair (see, e.g., Ref. [17]). Away from $X = 1$, the ninefold integral must be evaluated completely, but the three-body amplitude is not dominant and contributes at the same level as others: one enters into the land of uncertainties (off-shell extrapolations, high-momentum components, etc.) which I avoid in this report.

Not only the magnitude of the three-body, as well as the two-body, amplitudes are well under control in the quasielastic kinematics, but also the sharing of the momentum transfer between the three nucleon is responsible for the flattening of the cross section at high missing momenta in Fig. 1. The rise at the highest missing momentum reflects the increasing probability of forming a fast deuteron with two fast nucleons: this is only possible because their momentum mismatch is

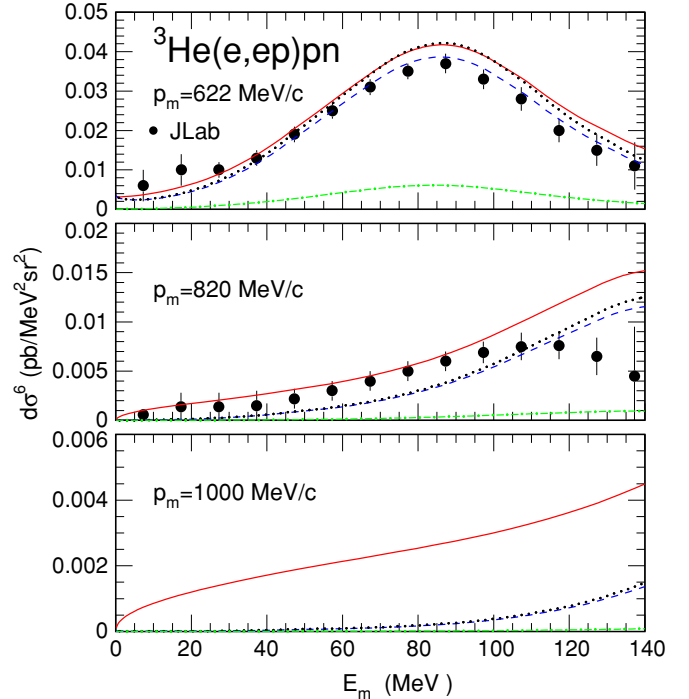


FIG. 4. (Color online) Missing energy distributions in the ${}^3\text{He}(e, e' p)np$ reaction at $X = 1$ and $Q^2 = 1.55$ GeV 2 for selected values of large missing momenta. Dash-dotted lines: PW. Dotted lines: FSI included. Dashed lines: two-body MEC and Δ production included. Full lines: three-body mechanisms included. The data are from Ref. [2].

strongly reduced in the three-body mechanisms, contrary to one- and two-body mechanisms (where one nucleon at least is almost spectator). The experimental confirmation of the high missing momentum part of the distribution is highly desirable. This can be best achieved by detecting the fast deuteron in coincidence with the electron (the Lorentz boost focuses more deuterons than protons in the detector). A preliminary result [18] confirms the prediction at $p_m \simeq 1.20$ GeV/c and confirms the trend of the $(e, e' p)$ data. A new experiment may use a third large acceptance magnetic spectrometer [19] in Hall A at JLab. One may also study the data already available at CLAS [20] in Hall B at JLab, if the statistics permits. Also, the determination of the angular distribution (Fig. 3) of the fast deuteron at constant missing momentum $p_m \sim 1$ GeV/c will map out the characteristic rapid variation of the three-body amplitude against X .

The virtual photon may also couple directly to two active nucleons which propagate before reinteracting with the third. However, such a mechanism is suppressed by the electromagnetic form factor of the pair, which falls down faster than the nucleon form factor when the virtuality Q^2 increases. Also, at $X = 1$, the kinematics prevents the proton from being emitted at rest, and consequently the photon interacts with a moving pair. A measure of these two effects is the strong reduction of the small backward peak (highest p_m) with respect to the forward peak ($p_m = 0$) in the plane wave curve of Fig. 1. On the contrary, the corresponding contributions are maximized at $X = 2$ since the proton can be

emitted at rest. Their experimental study remains to be done at high Q^2 .

Turning to the continuum, Fig. 4 shows typical missing energy (the internal energy E_m of the undetected pn pair) spectra at high recoil momentum (the total momentum p_m of the pn pair) in the ${}^3\text{He}(e, e'p)pn$ reaction [2]. At $p_m = 600$ MeV/c and below, the peak in the continuum emphasizes two nucleon mechanisms Refs. [3,21]. Its top corresponds to the kinematics of the disintegration of a pair of nucleons at rest, while its width reflects the Fermi motion of the spectator nucleon. Again, on-shell nucleon-nucleon rescattering dominates in the quasifree kinematics ($X = 1$) achieved in this experiment. The two-body MEC and Δ contribution suppresses the peak by about 10% at $p_m = 622$ MeV/c, but is smaller above. At higher missing momentum, this two-nucleon peak appears on top of a broad continuum, which is dominated by the nucleon Born part [Fig. 2(c)] of three-body mechanisms. It has been implemented according to Eq. (3) in the continuum three-body amplitude [22]. Besides the two other Born terms [Figs. 2(a) and (b)], it contains also the Δ formation term which is not forbidden by isospin selection rules. When integrated over the missing energy up to the pion threshold, the contribution of the three-body mechanisms reconciles the theoretical momentum distribution with the experimental one and gets rid of the discrepancy in Fig. 3 of Ref. [2] at high missing momenta.

In Fig. 4, the missing energy spectra have been plotted up to the pion production threshold, since the experiment has been performed with two magnetic spectrometers. To go beyond,

one needs to detect two nucleons in coincidence with the electron. This can be achieved with a third spectrometer [19] in Hall A or with CLAS [20] in Hall B at JLab.

The extension to the ${}^4\text{He}$ disintegration channels [23] would also be interesting since the relative importance of the two- and three-body mechanisms is expected to be different from ${}^3\text{He}$. For instance, the extra form factor in the amplitude of pion photoproduction on a pair of nucleons [see Fig. 4 and Eq. (5) in Ref. [10]] suppresses the contribution of the nucleon pole in the three-body mechanisms. But the presence of a fourth nucleon allows other mechanisms of which the amplitudes remain to be investigated.

In summary, this report completes the study of the electrodisintegration of ${}^3\text{He}$ which I undertook several years ago. As soon as the recoil momentum increases, nature prefers to share the momentum transfer first between two nucleons and then between the three nucleons, rather than to transfer it to a single nucleon [24]. This picture is on solid quantitative ground in the quasielastic kinematics ($X = 1$) where the singularity associated with the propagation of an on-shell nucleon maximizes the corresponding amplitudes. They depend on low-momentum components of the wave function and on on-shell elementary operators. It reproduces, without any free parameter over six decades, the beautiful textbook experiment recently performed at JLab. Far from the quasielastic kinematics, one enters into the domain where the tails of these amplitudes overlap and become less under control. One may wonder whether high-momentum components of the wave function will ever be accessible.

-
- [1] M. M. Rvachev *et al.*, Phys. Rev. Lett. **94**, 192302 (2005).
 [2] F. Benmokhtar *et al.*, Phys. Rev. Lett. **94**, 082305 (2005).
 [3] J. M. Laget, Phys. Lett. **B609**, 49 (2005).
 [4] R. Schiavilla *et al.*, private communication and to be published.
 [5] J. M. Laget, Phys. Rev. C **38**, R2993 (1988).
 [6] N. d'Hose *et al.*, Phys. Rev. Lett. **63**, 856 (1989).
 [7] J.-M. Laget, Phys. Rep. **69**, 1 (1981).
 [8] J.-M. Laget, Phys. Lett. **B151**, 325 (1985).
 [9] J.-M. Laget, Phys. Lett. **B199**, 493 (1987).
 [10] J.-M. Laget, Nucl. Phys. **A579**, 333 (1994).
 [11] M. Lacombe *et al.*, Phys. Lett. **B101**, 139 (1981).
 [12] Ch. Hajduk and P. U. Sauer, Nucl. Phys. **A369**, 321 (1981).
 [13] K. Aniol *et al.*, Phys. Rev. C **33**, 1714 (1986).
 [14] G. Backenstoss *et al.*, Phys. Rev. Lett. **55**, 2782 (1985).
 [15] I. Blomquist and J. M. Laget, Nucl. Phys. **A280**, 405 (1977).
 [16] J. M. Laget, Nucl. Phys. **A481**, 765 (1988).
 [17] J. M. Laget, J. Korean Phys. Soc. **26**, S244 (1993).
 [18] E. Voutier, in *Nuclear Theory*, Proceedings of the 23rd International Workshop on Nuclear Theory, Rila, Bulgaria, edited by S. Dimitrova (Heron Press, Sofia, 2004).
 [19] P. Monaghan, in *International Workshop on Probing Nucleons and Nuclei via the (e, e'p) Reaction*, edited by D. Higinbotham, J. M. Laget, and E. Voutier (Print House, New York, 2004), p. 253.
 [20] B. Mecking *et al.*, Nucl. Instrum. Methods A **503**, 513 (2003).
 [21] C. Ciofi degli Atti and L. P. Kaptari, Phys. Rev. C **71**, 024005 (2005).
 [22] J. M. Laget, J. Phys. G **62**, 1445 (1988).
 [23] K. Aniol *et al.*, JLab Experiment E01-108, 2001 (unpublished).
 [24] At the end of the review process of this manuscript, the paper nucl-th/0502045 by C. Ciofi degli Atti and L. Kaptari appeared. It offers an alternative explanation of the strength at high missing momentum, in terms of Glauber double scattering. The overlap between the two approaches remains to be evaluated.